Viscous Flow of Molten Polyethylene Resins*

HANS SCHOTT and W. S. KAGHAN

Film Division, Olin Mathieson Chemical Corp., New Haven, Connecticut

The flow behavior of molten polyethylene resins has been studied with rotational[4,13] and parallel plate viscometers[6] and piston- or gas-driven capillary rheometers.[1,2,9,12,19,21,22] Results obtained from different types of instruments are often in disagreement. During these measurements, the same resin sample is subjected to long heating times and sometimes also to long periods under shear. This often changes the flow characteristics of the resin prior to taking measurements.[1,9,22] Other sources of error of extrusion rheometers, such as the melt index apparatus, include large entrance losses,[12] friction due to shearing of melt between piston and barrel,[9] and a changing flow pattern as the piston approaches the die inlet.

In order to obtain valid data for the viscous flow of molten polyethylene resins covering the range of shear rates encountered in industrial processing, use was made of a screw extruder and a long capillary die. End effects were determined by comparison with shorter capillary dies. Apparent melt viscosities were measured as a function of shear and temperature.

Resins

Three commercial resins were studied, two of low density and one of high density. Their characteristics are listed in Table I.

TABLE I
Description of Resins

Designation	Resin type	Lot no.	Manufacturer	Density at 25°C.[a]	Melt index[b]	Intrinsic viscosity, dl./g.	Methyl groups/100 carbons[e]
Resin A	DYNH-3	5764	Union Carbide Plastics Co.	0.915	1.9	0.89[c]	3.3
Resin B	DFD-0114	G-1982	Union Carbide Plastics Co.	0.922	2.0	0.93[c]	2.6
Resin C	Marlex Series 6000 Type 50	2M-358	Phillips Chemical Co.	0.962	5.0	0.91[d]	<0.1

[a] Determined with pycnometer on samples annealed 30 min. in boiling water.
[b] Manufacturer's information.
[c] In toluene at 80°C.
[d] In α-chloronaphthalene at 125°C.
[e] By infrared absorption at 725 μ.

Equipment

A 2-in. Davis-Standard extruder was used. On the discharge side was a right angle elbow which reduced the 2-in. extruder opening to the 1-in. die

TABLE II
Dimensions of Dies

	Die inlet		Capillary		
Die	Height of conical frustrum, cm.	Included entry angle	Diameter, cm.	Length, cm.	Length/radius
C	1.90	60°	0.350	11.44	65.37
U	2.72	44°	0.366	5.82	31.80
H	2.51	45°	0.482	1.61	6.68
I	3.07	42°	0.356	0.00	0.00

* Presented at the Symposium on Rheology of Colloidal and Polymeric Systems, 137th Meeting of the American Chemical Society, Cleveland, Ohio, April, 1960.

inlet. Dies could be bolted interchangeably to the flange of the elbow. Die dimensions are listed in Table II. All dies comprised capillaries with streamlined inlets. Die I consisted only of a conical inlet, terminating in an orifice rather than a capillary.

Pressures were measured with Helicoid probe chemical gages (American Chain & Cable Co.), which were connected to the stream of melt by pressure taps. The gages were calibrated and maintained at 204 ± 2°C. during all experiments. One tap was directly above the die inlet, another in the reducing elbow. Their readings were in good agreement. Melt temperatures were measured with thermocouples in the elbow and just above the die inlet. The tip of the second thermocouple was positioned to give a temperature average for the 1-in. diameter cross section. The temperature of the melt issuing from the die was measured with a thermometer.

Treatment of Data

Flow rates were determined in duplicate by weighing the amount of extrudate collected during 2 min. periods. Pressure and melt temperature at the die inlet and melt temperature at the die exit were recorded before and after collecting each sample. Specific volumes necessary to convert weight to volume flow rates were calculated by eq. (16) of ref. 9. Maximum shear stresses and rates of shear at the wall were estimated by

$$\tau = PR/2L \tag{1}$$

and

$$D = 4Q/\pi R^3 \tag{2}$$

where P is the pressure drop, Q the volumetric flow rate, L the length, and R the radius of the channel.

Because of precise temperature controls, reproducibility of the data was good. Standard deviations for single determinations of apparent viscosity were less than 2%. Under extrusion conditions employed, the resins underwent no degradation.[17]

Equation (1) fits the flow of Newtonian and pseudoplastic systems, except that no allowance is made for entrance losses. Correction for entrance losses was made by assuming an effective capillary length greater than the actual length by a multiple (m) of the radius.[2,14] This gives an effective maximum shear stress

$$\tau_{ef} = PR/[2\ (L + mR)] \tag{3}$$

Kinetic energy corrections were insignificant.

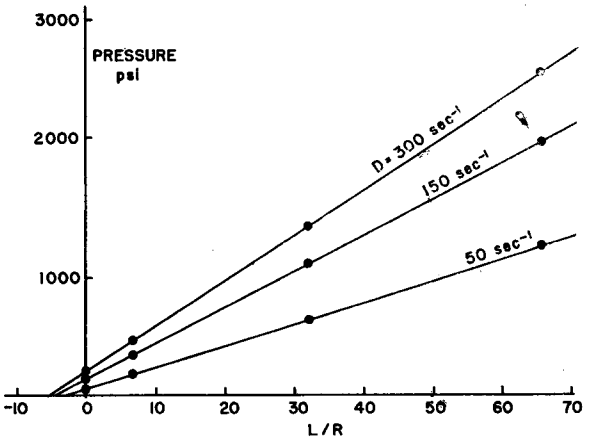

Fig. 1. Pressure vs. L/R at fixed shear rates, for Resin A at 150°C.

Equation (2) applies to Newtonian systems only. For the pseudoplastic melts, shear rates at the capillary wall were calculated by

$$\dot{\gamma} = \left(\frac{3 + n'}{4}\right) D \tag{4}$$

where n' is the slope of the log D–log τ plot.[8]

Logarithmic flow curves were often linear over wide ranges of shear rates. The linear portions can be represented by a power law[15]

$$D = K'\ \tau^{n'} \tag{5}$$

and

$$\dot{\gamma} = K\tau_{ef}^{\ n} \tag{6}$$

The two constants K and n characterize the resin at a given temperature. For Newtonian systems, $n = 1$ and K is the fluidity. The amount by which n exceeds unity shows how strongly non-Newtonian the system is. Where log $\dot{\gamma}$–log τ_{ef} plots were curved, shear stress and shear rate were correlated by a power series with even exponents,[15]

$$\dot{\gamma}/\tau_{ef} = a + b\ \tau_{ef}^2 + c\tau_{ef}^4 + d\tau_{ef}^6 \tag{7}$$

End Effects

In a very interesting paper,[2] Bagley showed that eq. (3) applied to the melt flow of low density polyethylenes. A straight line resulted when the pressure necessary to produce a given shear rate in a series of capillary dies of different L/R (length-radius) ratios is plotted against L/R. This line intersects the abscissa (P = 0) at $-m$:

$$P = 2\ \tau_{ef}(L/\ ) + 2m\tau_{ef} \tag{3A}$$

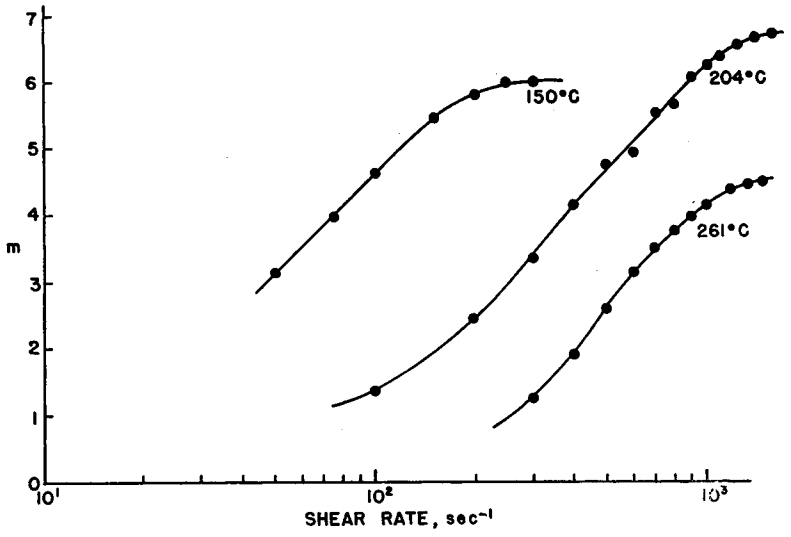

Fig. 2. End correction m for Resin A as a function of shear rate D.

The same linear relationship was observed in the present case, as shown in Figure 1 for Resin A at 150°C., and three levels of shear rate. This indicates that end effects are confined to the die inlet.

The m values calculated for Resin A at three temperatures are plotted against the corresponding shear rates in Figure 2. The curves are similar to Bagley's (Fig. 6 of ref. 2). According to Bagley, the inflection points mark the appearance of roughness and distortion in the extrudate, due to melt fracture or to another mechanism to relieve the stress caused by the abrupt convergence of flow lines at his 140° die inlet. Under our extrusion conditions, no extrudate irregularities were observed. This, however, does not rule out melt fracture at the die inlet. Our streamlined inlets (included angles 40–60°) prevent the accumulation of stagnant melt capable of wedging and causing pulsations. Therefore, shear fractures would heal rather than propagate to the die exit.[16]

The values of m as a function of shear rate are listed in Table III for the three resins at three temperatures. They increase with increasing rate of shear and with decreasing temperature. Under comparable conditions, Resin B has somewhat higher m values than Resin A, and both are considerably higher than those of Resin C.

The end effect consists of a purely geometric part m', the Couette correction which is common to Newtonian and non-Newtonian liquids, and of an elastic deformation in shear γ_{el}, the recoverable shear strain:

$$m = m' + (\gamma_{el}/2) \tag{8}$$

For Newtonian liquids, m' was found to be 0.6.[14]

The relative proportion of m' and $\gamma_{el}/2$ can be estimated by comparing the m values of Resins A and B with those of Resin C. The latter are so small that they should consist almost entirely of the geometric end effect. Consequently, the dif-

TABLE III
End Corrections m[a] for the Three Resins as a Function of Shear Rate

	Resin A			Resin B			Resin C		
D, sec.$^{-1}$	151°C.	204°C.	262°C.	151°C.	204°C.	262°C.	163°C.	218°C.	274°C.
100	4.6	1.4	—	6.4	—	—	—	—	—
200	5.8	2.5	—	6.8	5.0	2.0	0.8	—	—
300	6.0	3.3	1.2	7.1	5.8	3.2	1.3	—	—
500	—	4.8	2.6	—	6.4	4.3	2.1	1.6	1.1
700	—	5.5	3.5	—	6.7	5.2	—	1.6	1.1
1100	—	6.4	4.3	—	7.3	5.9	—	1.9	1.4
1500	—	6.8	—	—	—	6.3	—	—	1.7
2000	—	—	—	—	—	6.7	—	—	2.2

[a] m is defined by eq. (3).

ference in m of Resins A or B and m of Resin C is the lower limit for the recoverable strain portion of Resins A or B. Comparisons, made at the same temperature and at equally large deviations from Newtonian behavior, indicate that at least two-thirds to three-quarters of the end effect of Resins A and B is stored as shear strain.

The difference between the total energy input above the die inlet and the energy expended in overcoming the viscous friction of the melt in the same time interval provides a rough estimate of end effects. Total energy is calculated as the pressure-volume product. The energy dissipated by inner friction is converted into heat, and can therefore be estimated from the temperature increase of the melt between die inlet and exit. This requires that there be no heat exchange between melt and die. At high velocities, such heat exchange is negligible. The numerical example given in Appendix A shows the surprisingly close agreement between the end effect calculated by eq. (3) and by an energy balance.

The validity of eq. (3) and the reliability of this method of end correcting shear stresses is demonstrated by the fact that the same flow curves and viscosity relationships were obtained with all four dies, regardless of their L/R ratios. This is shown in Table IV for Resin A at 150°C., where the logarithmic flow curve was a straight line throughout the range studied. The four pairs of least squares values for the constants in the power law (last column) are equivalent. This is established by calculating end-corrected and uncorrected shear stresses at two levels of shear rate (center columns). At each D level, the four corrected shear stresses are practically identical.

TABLE IV
End Corrected Flow Characteristics of Resin A at 150°C. Determined with the Four Dies

Die, L/R	Shear stress, (dyne/cm.²) × 10^{-5}, at D = 30 sec.$^{-1}$ Uncorrected[a]	Corrected[b]	at D = 300 sec.$^{-1}$ Uncorrected[a]	Corrected[b]	Constants in power law[c] n'	$K' \times 10^{14}$
I (0.0)	—	5.39	—	12.81	2.66	1.70
H (6.7)	6.88	5.19	25.77	12.62	2.59	4.87
U (31.8)	6.17	5.31	18.31	12.45	2.70	1.05
C (65.4)	5.54	5.31	13.48	12.39	2.72	0.81

[a] Calculated by eq. (1).
[b] Calculated by eq. (3).
[c] Constants defined by eq. (6).

Uncorrected shear stresses are always greater than the corresponding corrected shear stresses. The difference becomes quite large for dies of small L/R. At an L/R of 6.7, uncorrected shear stress at 300 sec.$^{-1}$ and apparent viscosity based on it are twice as large as the corrected values. Despite their large magnitude, end corrections are often omitted in viscosity determinations even with relatively short dies.[3,9,11,19,21]

The data of Table IV indicate that, in the range of extrusion pressures employed, compressibility of the melt did not noticeably affect the apparent viscosity. The highest pressures used with dies C, U, H, and I were 3000, 1500, 500, and 300 psi, respectively.

Flow Relationships

Apparent melt viscosities were calculated from end-corrected maximum shear stresses and shear rates at the wall corrected for non-Newtonian behavior. Representative values are listed in Table V. The data confirm the well-known fact[4,6,9,13] that apparent viscosity decreases as shear and temperature increase. A tenfold increase in shear rate reduced the apparent viscosity to one-third or one-fourth of its initial value; a temperature rise of 66°C. reduced it to one-half.

TABLE V
Apparent Melt Viscosities of the Three Resins

Resin	$\dot{\gamma}$	Temperature, °C. 151	204	262
A	50 sec.$^{-1}$	11,200 poise	6,200 poise	3,200 poise
	500	2,640	1,730	1,070
B	50	12,950	7,210	3,840
	500	2,850	1,930	1,250
C	50	9,660	5,540	3,040
	500	3,140	1,930	1,360

Shear Dependence of Apparent Melt Viscosity is expressed by the difference between the exponent n in eq. (6) and unity. Values of n and K are listed in Table VI for approximately linear portions of the logarithmic flow curves (Figs. 3 and 4). The slopes are always greater than 45°. The degree of non-Newtonian flow behavior, $n - 1$, is seen to decrease with decreasing shear rate and/or with increasing temperature. At very low shear rates, melt flow is Newtonian.[1,13] Newtonian flow might even prevail at somewhat higher shear if high enough melt temperatures could be reached without decomposition.

TABLE VI
Melt Flow Characteristics: Constants in Power Law[a]

Resin	Temperature, °C.	Range of shear rate, sec.$^{-1}$	n	K
A	151	30–500[b]	2.692	1.68×10^{-14}
	204	70–700	2.226	3.04×10^{-11}
	262	180–1200	2.141	2.74×10^{-10}
B	151	25–400[b]	2.929	4.75×10^{-16}
	204	40–1000	2.336	5.23×10^{-12}
	262	100–500	2.048	6.62×10^{-10}
	262	500–1400	2.343	1.32×10^{-10}
	262	1400–3400	2.834	1.57×10^{-14}
C	163	40–500	1.924	7.47×10^{-10}
	218	40–250	1.636	7.68×10^{-8}
	218	250–1600	2.319	8.47×10^{-12}
	274	140–700	1.738	4.03×10^{-8}
	274	1000–2600	2.546	6.16×10^{-13}

[a] Equation (6).
[b] Applicable over entire range covered; may extend beyond.

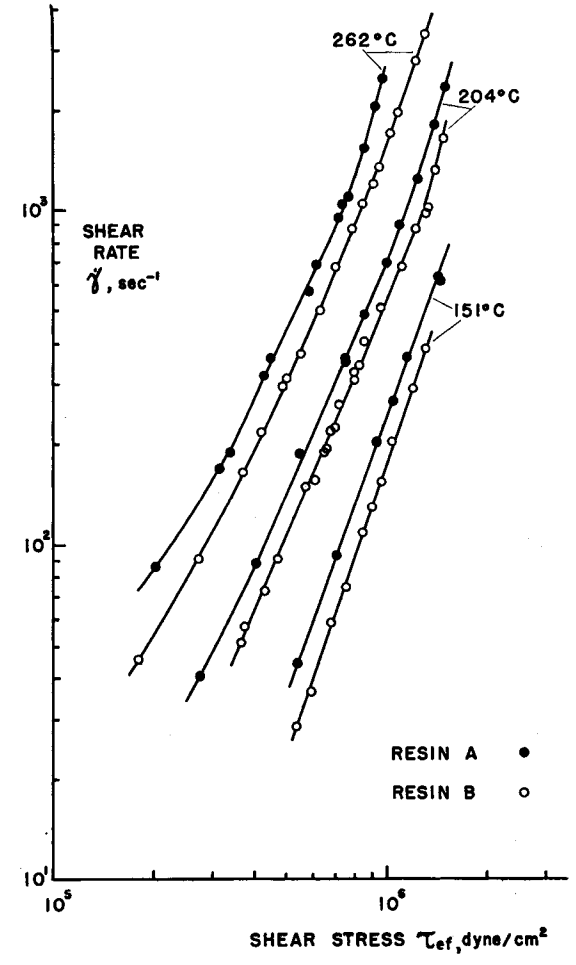

Fig. 3. Melt flow curves of Resins A and B.

At comparable shear rates and temperatures, Resin C has the smallest n value. This has also been observed at lower shear.[9] Marlex 50 had a value of θ (a measure of the shear dependence of flow) between one-half and one-fourth of θ values of commercial low density resins. The less non-Newtonian the flow behavior, the greater the curvature of the logarithmic flow curves.

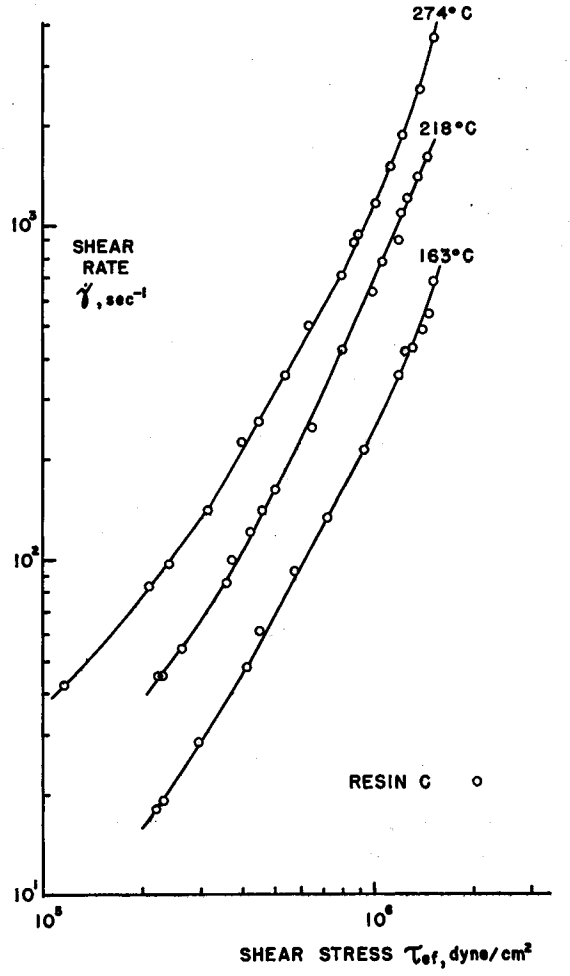

Fig. 4. Melt flow curves of Resin C.

Only for Resins A and B at 151°C. were the log $\dot{\gamma}$–log τ_{ef} plots linear over the entire range measured. The other flow data were fitted to eq. (7) by the method of least squares (see Table VII). Four terms were needed to reproduce the data adequately. When the exponent of shear stress in the power series was given the values 0, 1, 2, and 3, extrapolation beyond the experimental range introduced inflection points and minima in the flow curves. This seems to bear out Reiner's argument that only even powers be used.[15]

TABLE VII
Melt Flow Characteristics: Constants in Power Series[a]

Resin	Temperature, °C.	Value of constant a	b	c	d	Range of shear rate, sec.$^{-1}$
A	204	9.394×10^{-5}	8.502×10^{-16}	-3.546×10^{-28}	1.202×10^{-40}	50–2500
A	262	2.929×10^{-4}	2.899×10^{-15}	-3.189×10^{-27}	2.767×10^{-39}	75–3000
B	204	2.173×10^{-5}	9.010×10^{-16}	-5.647×10^{-28}	1.748×10^{-40}	50–2000
B	262	2.274×10^{-4}	1.604×10^{-15}	-3.925×10^{-28}	1.526×10^{-40}	50–3500
C	163	6.179×10^{-5}	3.530×10^{-16}	-2.103×10^{-28}	5.674×10^{-41}	20–800
C	218	1.808×10^{-4}	5.519×10^{-16}	-3.155×10^{-29}	-6.800×10^{-42}	40–1600
C	274	3.438×10^{-4}	1.254×10^{-15}	-5.893×10^{-28}	1.988×10^{-40}	40–4000

[a] Equation (7).

Temperature Dependence of Apparent Melt Viscosity is discussed in terms of apparent energy of activation for viscous flow ΔE, defined by the Arrhenius equation

$$\eta^* = Ae^{\Delta E/RT} \quad (9)$$

Since A is treated as a constant, ΔE for non-Newtonian systems is a function of shear rate or shear stress. According to the method of Bestul and Belcher, apparent activation energies for viscous flow were calculated at fixed rates of shear and at fixed shear stresses.[3] Plots of the logarithm of apparent viscosity at fixed $\dot{\gamma}$ or τ_{ef} versus the reciprocal of absolute temperature were often slightly curved; an average slope was then used to calculate ΔE. Results are given in Table VIII.

Zero shear activation energies were calculated by the method of Smallwood,[18] because extrapolation of apparent activation energies as a function of shear stress to zero shear involve large uncertainties. Moreover, extrapolated zero shear viscosities [e.g., from logarithm of apparent fluidity versus shear stress, or the reciprocal of constant a in eq. (7)] were much too low. For Resin A, initial viscosity values have been reported.[1] The zero shear activation energy calculated from these (12.1 kcal./mole) agrees with the value obtained by Smallwood's procedure (12.7 kcal./mole). The complete Smallwood treatment could not be applied because the value of A in his eq. (5),[18] related to the entropy of activation, decreases with increasing shear stress rather than remaining constant.

The zero shear activation energies of Resins A and B are in the 11.0–14.6 kcal./mole range reported for low density polyethylene.[1,4,6,9,10,13,20] The value of the high density Resin C is also in agreement with published values, which range from 6.5 to 7.5 kcal./mole and increase with the degree of branching.[10,20]

Apparent activation energies for viscous flow at fixed shear rates decrease as the level of shear rate increases. The value at 1000 sec.$^{-1}$ is one-third of the zero shear value. This effect is also shown by the slight but consistent convergence of plots of log η^* vs. log $\dot{\gamma}$ at different temperatures. The same observations have been made for the flow of polyethylene,[13] polyisobutylene, and GR-S rubber.[3]

Plots of log η^* vs. log τ at different temperatures

TABLE VIII
Apparent Activation Energies for Viscous Flow, kcal./mole

At fixed shear rates				At fixed shear stresses			
$\dot{\gamma}$, sec.$^{-1}$	Resin A	Resin B	Resin C	τ_{ef}, (dyne/cm.^{2}) $\times 10^{-5}$	Resin A	Resin B	Resin C
Zero shear	12.7[a]	11.6[a]	7.0[a]	Zero shear	12.7[a]	11.6[a]	7.0[a]
	12.1[b]				12.1[b]		
50	6.0	5.5	4.9	3.0	10.6	11.5	6.7
100	5.6	4.6	4.4	4.0	9.9	10.7	7.0
200	4.4	4.2	3.9	7.0	9.3	10.7	6.4
400	4.3	3.9	3.2	9.0	10.5	9.4	6.6
800	4.0	3.7	2.5	12.0	9.5	10.2	6.7
1600	3.9	3.1	2.2	15.0	9.5	—	7.2

[a] Extrapolated.[18]

[b] From measured initial viscosities.[1]

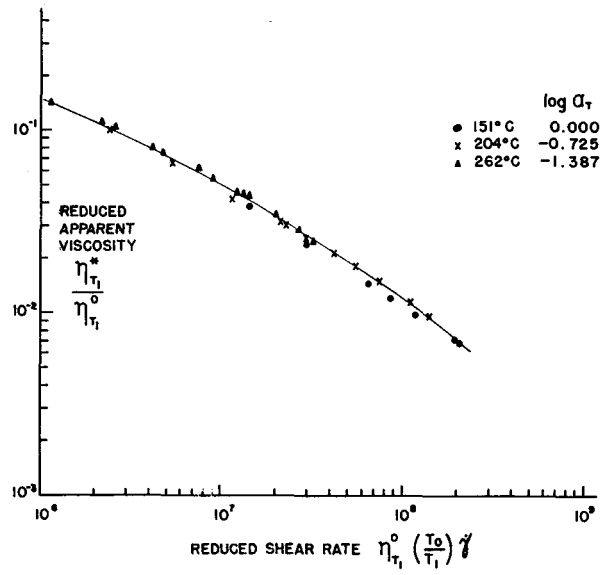

Fig. 5. Reduced steady state viscosity vs. reduced rate of shear for Resin A.

are approximately parallel: apparent activation energies at fixed shear stresses are independent of shear stress. As is seen in Table VIII, the variations of ΔE^*_τ with τ are small and without a trend. The same observation has been made with polyethylene,[4] polyisobutylene, and GR-S rubber.[3] Philippoff, on the other hand, found a consistent increase in ΔE^*_τ with τ for polyethylene: his activation energy increased by nearly 50% between zero shear and 10^6 dyne/cm.^{2}.[2,13]

As required by theory,[3] apparent activation energies at fixed shear stresses are always greater than at fixed shear rates. At comparable levels of shear stress or shear rate, Resin C always had the smallest apparent activation energies.

De Witt has extended Ferry's method of reduced variables to steady flow viscosity of non-Newtonian systems: the variable was reduced rate of shear instead of reduced frequency.[5] In Figure 5, initial melt viscosities of Resin A[1] are combined with present high shear data on a plot of reduced apparent viscosity versus reduced rate of shear. The points for three temperatures fall on a single curve.

Discussion

An attempt is made below to interpret the observed differences between the melt flow characteristics of the high and the low density polyethylene in terms of structure.

The structural differences between the two types of resin are as follows (see Table I): The two low density resins have a considerable amount of short and long chain branching, the high density resin little or none. Weight-average molecular weights, calculated from intrinsic viscosities, are 178,000 for Resin A, 188,000 for Resin B, and 92,000 for Resin C. Molecular weight distributions are probably much broader for the low density resins. Approximate ratios of weight-average to number-average molecular weight are 58 for Resin A and 10 for Resin C.

The first rheological difference is that the apparent melt viscosities of Resins A and B decrease faster with increasing shear than that of Resin C. This is tentatively attributed to the narrower molecular weight distribution of the latter, a factor which has been shown to lead to less non-Newtonian melt flow behavior in polystyrene and polyethylene resins.[11,20]

The second rheological difference is the smaller temperature coefficient of the apparent melt viscosity of Resin C. The high density resin has no short chain branching whereas the low density resins have branches several carbon atoms long spaced on the average 30 to 40 carbon atoms apart. These branches render the chains of Resins A and B less flexible and increase the size of the flow unit. This, in turn, requires larger holes for flow and hence a greater activation energy for the low density resins.

The third rheological difference is the smaller end effect in the melt flow of Resin C, due to low recoverable shear strain. In the molten state, molecules of the low density resins are more compact than molecules of the high density resin because of branching. The linear molecules of Resin C are therefore more entangled. If each point of entanglement is considered a temporary crosslink, there is a higher density of crosslinks in the melt of the high density resin. According to the theory of rubber elasticity, this melt then has a higher modulus of rigidity, and a given shearing stress will produce a smaller elastic deformation in the melt of Resin C than in the melts of Resins A and B.

APPENDIX A: NUMERICAL CALCULATION OF END EFFECTS

Extrusion Conditions

Resin B, Die C, Q = 3.25 cm.^{3}/sec., D = 772 sec.$^{-1}$, P = 2250 psi = 1.55×10^8 dyne/cm.^{2}; melt temperature 438°F. above die inlet and 450°F. at die exit; temperature rise = 12°F. = 6.7°C.

End Effects by Energy Balance

Rate of overall energy input is PQ = (1.55 × 10^8 dyne/cm.^{2}) (3.25 cm.^{3}/sec.) = 5.04 × 10^8 erg/sec. = 12.04 cal./sec.

Rate of generation of frictional heat is $Qc\Delta T$, where c is specific heat per unit volume. The specific heat at 229°C. is 0.682 cal./g./°C.,[7] the specific volume 1.3586 cm.^{3}/g.[9] Hence, c = 0.502 cal./cm.^{3}/°C. $Qc\Delta T$ = (3.25 cm.^{3}/sec.) (0.502 cal./cm.^{3}/°C.) (6.7°C.) = 10.93 cal./sec. Entrance loss is thus 12.04 − 10.93 = 1.11 cal./sec., or 9.2% of the total pressure drop.

End Effects According to Equation 3

τ = 1.187 × 10^6 dyne/cm.^{2} [by eq. (1)], m = 6.2 and τ_{ef} = 1.084 × 10^6 dyne/cm.^{2} [by eq. (3)]. End effects are the difference between total and effective shear stress (1.187 − 1.084) × 10^6 dyne/cm.^{2} = 0.103 × 10^6 dyne/cm.^{2}, or 8.7% of total shear stress.

References

1. Aggarwal, S. L., L. Marker, and M. J. Carrano, *J. Appl. Polymer Sci.*, **3,** 77 (1960).
2. Bagley, E. B., *J. Appl. Phys.*, **28,** 624 (1957).
3. Bestul, A. B., and H. V. Belcher, *J. Appl. Phys.*, **24,** 696 (1953).
4. Dexter, F. D., *J. Appl. Phys.*, **25,** 1124 (1954).
5. De Witt, T. W., *J. Appl. Phys.*, **26,** 889 (1955).
6. Dienes, G. J., and H. F. Klemm, *J. Appl. Phys.*, **17,** 458 (1946).
7. Dole, M., et al., *J. Chem. Phys.*, **20,** 781 (1952).
8. Krieger, I. M., and S. H. Maron, *J. Appl. Phys.*, **25,** 72 (1954).
9. Marker, L., R. Early, and S. L. Aggarwal, *J. Polymer Sci.*, **38,** 381 (1959).
10. Marshall, D. I., Abstracts of Papers, 130th Meeting, American Chemical Society, Atlantic City, N. J., September 1956, p. 18S.
11. McCormick, H. W., F. M. Brower, and L. Kin, *J. Polymer Sci.*, **39,** 87 (1959).
12. Merz, E. H., and R. E. Colwell, *ASTM Bulletin No.* **232,** 63 (1958).
13. Philippoff, W., and F. H. Gaskins, *J. Polymer Sci.*, **21,** 205 (1956).
14. Philippoff, W., and F. H. Gaskins, *Trans. Soc. Rheology*, **2,** 263 (1958).
15. Reiner, M., *Deformation, Strain and Flow*, Interscience, New York, 1960.
16. Schott, H., and W. S. Kaghan, *Ind. Eng. Chem.*, **51,** 844 (1959).
17. Schott, H., and W. S. Kaghan, *Modern Plastics*, **37,** No. 7, 116 (1960).
18. Smallwood, H. M., *J. Appl. Phys.*, **8,** 505 (1937).
19. Tordella, J. P., *SPE Journal*, **9,** No. 5, 6 (1953).
20. Tung, L. H., American Chemical Society, Division of Polymer Chemistry, Papers presented at Cleveland Meeting, **1,** No. 1, 14 (April 1960).
21. Westover, R. F., *Processing of Thermoplastic Materials*, ed. by E. C. Bernhardt, Reinhold, New York, 1959, pp. 590–627.
22. Westover, R. F., and B. Maxwell, *SPE Journal*, **13,** No. 8, 27 (1957).

Synopsis

A screw extruder and capillary dies of different length-radius ratios were used to measure melt flow and end effects for three commercial polyethylene resins, two of low density and one of high density. The apparent melt viscosities of the low density resins decreased faster with increasing shear and temperature than that of the high density resin. Zero shear activation energies for viscous flow were 11.6 and 12.7 kcal./mole for the low density resins and 7.0 for the high density resin. Apparent activation energies at fixed shear stresses were independent of shear stress while apparent activation energies at fixed shear rates decreased with increasing shear rate. End effects and recoverable shear strain were smallest for the high density resin. The differences between the melt flow characteristics of the two types of polyethylene are tentatively correlated with structure.

Résumé

Un extrudeur hélicoïdal et des capillaires de différentes rayons ont été employés pour mesurer l'écoulement à l'état fondu et les effets des extrémités sur 3 résines commerciales de polyéthylène; deux de faible densité et une de haute densité. Les viscosités apparentes des résines de basse densité diminuent plus rapidement avec l'augmentation du cisaillement et de la température que celle de la résine de haute densité. Les énergies d'activation à cisaillement nul pour un écoulement visqueux, sont respectivement de 11,6 à 12,7 Kcal/mole pour les résines de basse densité et 7 pour la résine de haute densité. Les énergies d'activation apparentes pour des tensions de cisaillement fixées sont indépendantes de la tension de cisaillement, alors que les énergies d'activation apparentes pour des vitesses de cisaillement déterminées diminuent avec l'augmentation de la vitesse de cisaillement. Les effets des extrémités et la force de recouvrement sont les plus faibles pour la résine de haut densité. Les différences entre les caractéristiques d'écoulement des 2 types de polyéthylène sont expérimentalement mis en corrélation avec la structure.

Zusammenfassung

Ein Schraubenextruder und Kapillarmatrizen mit verschiedenem Länge-Radiusverhältnis wurden zur Messung des Schmelzfliessens und von Endeffekten an drei handelsüblichen Polyäthylenharzen, zwei mit niedriger und eines mit hoher Dichte, verwendet. Die scheinbare Schmelzviskosität der Harze niedriger Dichte nahm mit wachsendem Schub und wachsender Temperatur rascher ab, als diejenige der Harze hoher Dichte. Die Aktivierungsenergien beim Schub Null für das viskose Fliessen betrugen 11,6 und 12,7 kcal/Mol für das Harz niedriger Dichte und 7,0 für das Harz hoher Dichte. Scheinbare Aktivierungsenergien bei bestimmten Schubspannungen erwiesen sich als unabhängig

von der Schubspannung, während scheinbare Aktivierungsenergien bei bestimmter Schubgeschwindigkeit mit wachsender Schubgeschwindigkeit abnahmen. Endeffekte und reversible Schubverformung waren bei den Harzen hoher Dichte am kleinsten. Die Unterschiede in der Charakteristik des Schmelzfliessens der beiden Polyäthylentypen werden versuchsweise zu ihrer Struktur in Beziehung gebracht.

Received August 24, 1960